Dissociable corticostriatal circuits underlie goal-directed versus cue-elicited habitual food seeking after satiation: Evidence from a multimodal MRI study

Henk van Steenbergen[1,2], Poppy Watson[3,4], Reinout W. Wiers[3,5], Bernhard Hommel[1,2], & Sanne de Wit[3,4]

1. Leiden Institute for Brain and Cognition, The Netherlands
2. Leiden University Institute of Psychology, The Netherlands
3. Amsterdam Brain and Cognition, University of Amsterdam, The Netherlands
4. Department of Clinical Psychology, University of Amsterdam, The Netherlands
5.Addiction Development and Psychopathology (ADAPT) lab, Department of Developmental Psychology, University of Amsterdam, The Netherlands

In press at
European Journal of Neuroscience

Corresponding author:
Henk van Steenbergen
Wassenaarseweg 52
2333 AK Leiden
The Netherlands
Phone number: +31 (0)71 527 3655
Fax number: +31 (0)71 527 3783
E-mail address: HvanSteenbergen@fsw.leidenuniv.nl

Author contributions:
All authors were involved in the design of this study. HvS performed data collection and analyses. HvS, PW and SdW interpreted the data and wrote a first draft of the article. All authors provided critical revisions.

Acknowledgements:

We thank dr. John O'Doherty for his valuable input on an earlier version of this paper. We are grateful to Christina Pfeuffer for her invaluable help in setting up this study. We thank Nienke Pannekoek and Jelle van Leusden for their help in data acquisition and Wouter Weeda for his advice on the analyses. This research was made possible by funding received from the Netherlands Organization for Scientific Research (NWO; 433-09-243).

Keywords:
Decision-making; Goal-directed behavior; Habitual behavior; Pavlovian-Instrumental Transfer; Food-seeking; Corticostriatal circuits; Functional Magnetic Resonance Imaging; Diffusion Tensor Imaging;Voxel-Based Morphometry

Word count: 8813 (Main text)

Abstract

The present multimodal MRI study advances our understanding of the corticostriatal circuits underlying goal-directed versus cue-driven, habitual food seeking. To this end, we employed a computerized Pavlovian-instrumental transfer (PIT) paradigm. During the test phase, participants were free to perform learnt instrumental responses (left and right key presses) for popcorn and Smarties outcomes. Importantly, prior to this test half of the participants had been sated on popcorn and the other half on Smarties – resulting in a reduced desirability of those outcomes. Furthermore, during a proportion of the test trials, food-associated Pavlovian cues were presented in the background. In line with previous studies, we found that participants were able to perform in a goal-directed manner in the absence of Pavlovian cues, meaning that specific satiation selectively reduced responding for that food. However, presentation of Pavlovian cues biased choice towards the associated food reward regardless of satiation. Functional MRI analyses revealed that, in the absence of Pavlovian cues, posteriorventromedial prefrontal cortex tracked outcome value. In contrast, during cued trials, the BOLD signal in the posterior putamen differentiated between responses compatible and incompatible with the cue-associated outcome. Furthermore, we identified a region in ventral amygdala showing relatively strong functional connectivity with posterior putamen during the cued trials. Structural MRI analyses provided converging evidence for the involvement of corticostriatal circuits: diffusion tensor imaging data revealed that connectivity of caudate-seeded white-matter tracts to the ventromedial prefrontal cortex predicted responding for still-valuable outcomes; and gray matter integrity in the premotor cortex predicted individual Pavlovian cueing effects.

Introduction

When sated on a particular food, humans and other animals typically no longer attempt to obtain that food, indicating that the behavior is under the control of reward expectancy and evaluation of its current desirability. In that case, behavior meets the cognitive and motivational criteria of goal-directed behavior as described by Dickinson and colleagues (de Wit & Dickinson, 2009; Heyes & Dickinson, 1990; but for an alternative definition of goal-directed behavior see Hommel, 2015). However, under certain conditions - most notably, following prolonged repetition of the food-seeking behavior - food seeking will become habitual and will consequentially continue despite satiation (Adams, 1982; Colwill & Rescorla, 1985, 1988). To explain this loss of behavioral flexibility, dual-process models of action selection propose that with repetition a transition takes place from flexible, value-driven goal-directed behavior towards predominantly cue-driven habits that are triggered independently of the current desirability of the outcome (Dickinson *et al.*, 1995; de Wit & Dickinson, 2009; Balleine & O'Doherty, 2010; Hogarth & Chase, 2011; Huys *et al.*, 2011; Hogarth, 2012).

An experimental model of cue-driven instrumental choice behavior is provided by the (outcome-specific) Pavlovian-instrumental transfer (PIT) paradigm, which was originally developed in animal research (Estes, 1948; Colwill & Rescorla, 1988a) and more recently translated to humans (Bray *et al.*, 2008; Allman *et al.*, 2010; Hogarth & Chase, 2011; Prevost *et al.*, 2012; Watson *et al.*, 2014; Eder & Dignath, 2015). The idea behind this paradigm is that reward-associated cues will tend to trigger behaviors that are associated with those rewards. For example, the influence of commercials and adverts on food seeking and consumption (see e.g., Harris, Pomeranz, Lobstein, & Brownell, 2009) could be mediated by such a mechanism. To

illustrate, the well-known golden arches could remind one of cheeseburgers, which could in turn inspire a visit to McDonald's to purchase one.

To study this form of cue-driven behavior, a typical PIT task consists of three separate stages (see Figure 1 for an example). In the first (instrumental) stage, participants learn to respond (R) for certain outcomes (O), which should lead to the formation of O-R associations (e.g., Smarties → left key press; popcorn → right key press). In the second (Pavlovian) stage, they learn to associate a set of neutral stimuli (S) with the same outcomes as in instrumental training, leading to S-O associations (e.g., triangle → Smarties; circle → popcorn). In the final transfer test phase, the effect of stimulus presentation on action selection is tested. Many studies have shown that the Pavlovian cues tend to bias responding in the direction of the signaled outcome (e.g., an increase in responding for chocolate when the triangle is presented), implying cue-driven behavior that is mediated by indirect S-O-R associations (see Figure 1C for an illustration).

The question arises whether the cue-driven behavior in the PIT paradigm provides a model of habitual behavior, in the sense that the cued behavior is insensitive to current outcome value. In support of this idea, several studies have observed that actions driven by Pavlovian cues are resistant to devaluation of the outcome through for example satiation, both in rodents (Colwill & Rescorla, 1990; Rescorla, 1994; Holland, 2004; Corbit *et al*., 2007) and humans (Hogarth et al., 2012; Hogarth & Chase, 2011; Watson et al., 2014; for notable exceptions, see Allman et al., 2010; Eder & Dignath, 2015). Because of this lack of immediate sensitivity to changes in the motivational significance of an outcome, PIT is thought to be mediated mainly by the sensory as opposed to hedonic features of the outcome (see Delamater & Oakeshott, 2007). The sensory features of the outcomes signaled by the Pavlovian stimulus are likely encoded in ventral amygdala (Balleine & Killcross, 2006) as was recently confirmed in a high-resolution functional

magnetic resonance imaging (fMRI) in humans (Prevost *et al.*, 2012). In turn, the posterior putamen **has been implicated in overtrained, habitual responding that is insensitive to devaluation (Tricomi *et al.*, 2009) but also to the PIT effect (Bray *et al.*, 2008).**

The aim of the present study was to replicate and extend the available evidence on the neural mechanisms underlying Pavlovian cue-driven action **control (via sensory outcome representations) and to compare it directly with value-driven, goal-directed actions in the absence of a cue. To this end, we used a modified version of a combined PIT/outcome devaluation paradigm that was recently employed by our group (Watson *et al.*, 2014). This experimental design measures instrumental responses for food rewards in the presence and absence of food-associated cues, allowing us to identify brain regions specifically involved in cue-driven behavior. Furthermore, in order to reveal regions involved in value-driven behavior, value will be manipulated by sating participants selectively on one of the food rewards.** With regard to the behavioral results, we expect to replicate the findings by Watson and colleagues (Watson *et al.*, 2014), who showed that satiation reduces responding for the devalued food outcome in the non-cued condition (indicating action selection based on expected value) but does not affect outcome-specific transfer in the cued conditions (indicating action selection driven by the cue). We adopt a multimodal MRI approach to investigate neural activity as well as individual differences in brain structure that underlie uncued goal-directed versus cued habitual behavior. The functional MRI analyses aimed to directly compare neural activity related to responding for valuable (versus devalued) outcomes in the presence and absence of outcome-associated stimuli (during cued and non-cued trials, respectively). We hypothesized that goal-directed actions during non-cued trials should involve the ventromedial prefrontal cortex (vmPFC), as observed in previous studies (Gottfried *et al.*, 2003; Valentin *et al.*, 2007; de Wit *et al.*, 2009; Gläscher *et al.*, 2009). On the other hand, we expected that outcome-specific transfer

during cued trials should involve the posterior putamen and ventral amygdala, **in line with the idea that PIT provides a mechanism for cue-driven, habitual responding(Bray *et al.*, 2008; Prevost *et al.*, 2012)**. The structural MRI analyses were conducted to test the prediction that individual differences in value- and cue-driven behavior relate to dissociable corticostriatal white matter connectivity and gray matter integrity (Balleine & O'Doherty, 2010) as identified by Diffusion Tensor Imaging (DTI) tractography and Voxel-Based Morphometry (VBM), respectively. **Support for two dissociable corticostriatal networks comes indirectly from studies that have used white matter tractography to reveal connections between vmPFC and caudate, and between posterior putamen and premotor cortex (Lehéricy *et al.*, 2004; Draganski *et al.*, 2008). Furthermore, one study reported that the estimated strength of these anatomical connections was related to individual differences in the balance between flexible, goal-directed behavior and habitual responding, respectively (de Wit *et al.*, 2012; for partial replication, see Delorme *et al.*, 2016). Here, w**e tested for the first time whether goal-directed action (during the non-cued trials) and habitual responding (during the cued PIT trials) were related to neural integrity in these caudate-vmPFC and posterior putamen-premotor cortex circuits, respectively.

Materials and Method

Participants

Thirty healthy right-handed volunteers (age 18–28 years; 6 males) with normal vision and no dental braces participated in the study. We did not control for the menstrual cycle phase of the female subjects. All participants were asked to refrain from eating for at least two hours before the start of the experiment. The volunteers gave written informed consent and they were paid 25 euros for participation in this experiment which took about 90 minutes in total. The experiment

was approved by the medical ethics committee of the Leiden University Medical Center. Six participants were excluded from further analyses because they scored at or below 50% chance level on the instrumental query trials presented after the test phase, which indicated a failure to learn the correct response-outcome association between the two response keys and the popcorn and Smarties outcomes. One other participant was also excluded because of a failure to respond to the no-outcome stimulus. In addition, due to a technical issue, scanning data were not stored for one other participant.

Of the remaining 22 participants (4 males) used for the behavioral analysis, three participants were excluded for the functional MRI analysis on goal-directed behavior to preclude empty cells in the event-related model (these participant never preferred the devalued response during the non-cued trials). All other fMRI analyses included this same set of 19 participants (4 males), except for: the functional MRI analysis on outcome-specific transfer which excluded an additional eight participants (these participants never made an incongruent response to the valued and/or devalued cue) resulting in 11 participants (4 males) being included for analysis; and the functional connectivity analysis which excluded an additional three participants (these participants never made any incongruent response when collapsing valued and devalued cues) resulting in 16 participants (4 males) being included for analysis. For the structural MRI analyses, one participant out of the 22 participants was excluded because of a technical issue with the DTI acquisition.

Study Procedure and Pavlovian-Instrumental Transfer (PIT) task

We replicated a study design recently developed by Watson et al. (2014). We used real food outcomes: mini chocolate Smarties (Nestle, 471 calories per 100 g), and salted popcorn (Albert Heijn, 525 calories per 100 g). The study consisted of instrumental and Pavlovian training

phases and a satiation manipulation outside the scanner (Figure 1A) followed by a test phase inside the scanner (Figure 1C). At the start of the experiment, participants sampled the Smarties and popcorn and rated on Likert scales how much they desired eating each food (T0). They were also asked to rate their hunger. The participants performed the training phases in a supine position with a head coil and viewed the stimuli through a mirror, thus mimicking the subsequent test phase in the MRI scanner.

Phase 1: Instrumental Training (R-O learning). Upon presentation of a purple box in the center of the screen (the availability window), participants could press on one of two keys using one finger of their right hand to obtain popcorn or Smarties (response–outcome relationship counterbalanced). Participants were instructed that on each trial only one of the two food outcomes would be available which was to be learned by trial and error. They were instructed to continue trying both keys until they won something – indicated by a popcorn or Smarties image on the screen. Participants were asked to try and learn the relationships between the keys and the food outcomes and were told that they occasionally would be tested on this. The amount of specific key presses needed to show the image of the food outcome available on that trial was determined by a variable ratio schedule of 10 ± 5 presses. The image remained on the screen for 1 s and then was followed by a 1.5 s inter-trial interval (ITI) during which the box turned dark grey. Every fourth time that a specific food image was presented, a sound indicated that the experimenter would provide the participant one piece of that food (popcorn or chocolate Smartie) to be consumed immediately. The ITI was 6s after these ‘eating’ trials. The instrumental training phase presented four blocks in which the two different food outcomes were both available three times, in random order (24 trials in total). The screen background was always a black and white checkerboard and all stimuli were overlaid on this background. The checkerboard used the same distribution of black/white pixels as the stimuli to ensure matched luminance. At the end of the

second and fourth instrumental blocks, four instrumental query trials (each food outcome presented twice in random order) were presented to test the knowledge about response-outcome contingencies. On each query trial a picture of either popcorn or Smarties was presented, upon which the participant was asked to press the key that previously yielded that food outcome. After participants pressed a key, they received feedback on their choice by presentation of the words 'correct' or 'incorrect' for 2s, which was followed by a 0.5-s ITI.

Phase 2: Pavlovian Training (S-O learning). This phase involved learning the relationships between three counterbalanced Pavlovian cues (black and white patterns) and three different food outcomes (popcorn, Smarties, or no-outcome) while participants passively viewed the screen. They were asked to pay attention because they would be occasionally tested on their knowledge of the relationships between the patterns and the food outcomes. During each trial, one of the three Pavlovian cues was presented for 2s, and was then overlaid with the picture of the food (or the word "nothing") outcome for 1s. The ITI was 1.5s. during which a fixation cross was presented in the middle of the screen. Every fourth time that a specific food outcome picture was presented, a sound signaled that during the subsequent 6-s ITI the participant should consume a piece of that food that was presented by the experimenter. The Pavlovian training phase contained four blocks. During each block the three cues were presented three times in random order (36 trials in total). At the end of the second and fourth block, Pavlovian query trials tested the participants on their knowledge of the cue–outcome contingencies. On each query trial, one of the Pavlovian cues was presented, upon which the participant had to select the picture of the outcome that had followed this cue using a mouse. Participants received feedback by presentation of the words 'correct' or 'incorrect' for 2s along with the image of the correct food outcome that had been signaled by the cue. During each block of query trials the three cue-outcome combinations were presented twice in random order (six trials in total).

Phase 3: Satiation Manipulation. Following these training phases, participants were seated in a comfortable chair and filled in hunger and food wanting ratings for the second time (T1). Then participants watched 10 minutes of the Series 1 Episode 2 of the popular American TV show "Modern Family" while trying to eat 100 grams of either smarties or popcorn (type of satiated food counterbalanced across subjects). Subsequently, the participants completed the hunger and food wanting ratings again (T2) and rated how much they enjoyed watching the show.

Phase 4: Non-cued and Cued Test Trials. Participants were brought to the MRI scanner where the test phase of the PIT task was run immediately after a reference scan of the brain was made. During this test phase participants were free to respond on the popcorn and Smarties keys as often as they liked in order to win these food outcomes. No food was in sight during this phase of the task. During the non-cued trials, we assessed choice behavior in the absence of Pavlovian cues to see whether participants would respond in a value-directed manner (i.e. try to win food outcomes they had not been sated on). During the cued trials, we assessed whether presentation of the different Pavlovian cues would bias responding on different keys (via S-O-R associations).

Before the test phase started, participants were instructed that they could push on either key as often as they liked in order to win popcorn or chocolate Smarties during 3-s periods in which a purple box was presented. They were told that, as before, only one of the two food outcomes would be available on each trial but that this time they would not be told after each trial which food they had won. Instead, they would find out at the end of the test phase how many Smarties or pieces of popcorn they had earned and they would then eat these. **The test was therefore conducted in nominal extinction. Discontinuing to present the (devalued and still-valuable) outcomes contingent upon responding in the test phase is crucial in order to prevent novel learning. Outcome-devaluation as well as PIT studies therefore typically**

conduct the critical test phase in extinction, to allow investigation of *immediate* adjustments of choice behavior on the basis of value (as manipulated by satiation) and cues (as measured on uncued versus cued PIT trials).Participants were instructed that they would occasionally see patterns appear on the screen but they should primarily focus on the purple box indicating the availability to respond for food outcomes. The test trials were presented in ten blocks with two trials of each of the three Pavlovian cues and two non-cued trials, in random order (amounting to 80 trials in total). During each inter-trial interval (jittered duration between 2.2s and 8.2s.), the screen contained a black and white checkerboard which was overlaid by a grey box. After this inter-trial interval, the grey box turned purple for 3 seconds, and the background either changed into a checkerboard with flipped colors (non-cued trials) ór presented one of the Pavlovian background cues (cued trials).

After receiving the above instructions, participants first received five demo non-cued trials. After the demo, the test trials were presented while EPI scans were acquired and the number of presses on each key was recorded. At the end of the test phase, a block of four instrumental query trials tested whether the participants remembered the instrumental response–outcome relationships from the instrumental training session. The timing was the same as reported previously, but the participants did not receive feedback on these query trials. Following the scan session of anatomical scans, participants received their earned food rewards, weight and height were measured and the participant was paid and thanked for participation.

Behavioral analyses

We conducted repeated-measures ANOVAs on data that were labeled in terms of valued and (to-be) devalued outcomes/responses/cues. The between-subjects factor satiation group coded whether participants were satiated on chocolate or popcorn**. All within-subject factors**

used for the specific analyses are mentioned in the respective Results sections. Greenhouse-Geisser correction was applied when assumptions of sphericity were violated. In these cases, we report corrected p-values along with the original degrees of freedom. All significant effects ($p < 0.05$) are reported. We also report t-tests for subsequent planned comparisons. Pearson correlations between self-report data and behavioral indices are also reported (see Results). We report two-tailed p-values throughout the paper.

MRI Data Acquisition

Scanning was performed with a standard whole-head coil on a 3-T Philips Achieva MRI system (Best, The Netherlands) in the Leiden University Medical Center. During the task, 312 T2*-weighted wholebrain EPIs were acquired, including 2 dummy scans preceding the scan to allow for equilibration of T1 saturation effects (TR = 2.2 s; TE = 30 ms, flip angle = 80°, 38 transverse slices, 2.75 × 2.75 × 2.75 mm +10% interslice gap). Stimuli were projected onto a screen that was viewed through a mirror at the head end of the scanner. After the functional runs, a high-resolution EPI scan (TR = 2.2 ms; TE =30ms, flip angle = 80°, 84 transverse slices, 1.964 × 1.964 × 2 mm) and a B0 field map were acquired for registration purposes. This was followed by a 3D T1-weighted scan (TR = 9.8 ms; TE = 4.6 ms, flip angle = 8°, 140 slices, 1.166 × 1.166 × 1.2 mm, FOV = 224.000 × 177.333 × 168.000) and a diffusion-weighted scan using spin-echo echo planar imaging (TR = 7.316 s; TE = 69 ms; 75 2 -mm-thick axial slices; matrix size 128 × 128; in-plane resolution, 1.875 × 1.875 mm^2). DTI data were acquired in two scans in an anterior-to-posterior and posterior-to-anterior direction. Both scans were acquired along 30 directions and also included a baseline image having no diffusion weighting (b = 0).

fMRI Preprocessing

FMRI data analysis was carried out using FEAT (FMRI Expert Analysis Tool) Version 5.98, part of FSL (FMRIB's Software Library, www.fmrib.ox.ac. uk/fsl) (Smith *et al.*, 2004). The following pre-statistics processing was applied: motion correction, B0 unwarping, brain extraction, spatial smoothing using a Gaussian kernel of FWHM 8.0 mm, grand-mean intensity normalization of the entire 4D dataset by a single multiplicative factor, high-pass temporal filtering (Gaussian-weighted least-squares straight line fitting, with sigma = 60.0 s). In native space, the fMRI time series were analyzed using an event-related approach in the context of the general linear model with local autocorrelation correction. The different models used to test our hypotheses are described in detail below. All models were high-pass-filtered (Gaussian-weighted least-squares straight-line fitting, with sigma = 60.0 s). For all models, the trial type regressors used square-wave functions to represent stimulus duration and were convolved with a canonical HRF and its temporal derivative. After confirming that individual runs were registered correctly and did not indicate excessive motion, the relevant COPE images were transformed to standard space via a high-resolution EPI image and T1 image (using FLIRT) and were then merged into a single 4D file for statistical analyses.

Specification of fMRI models to test brain-activity hypotheses

Role of vmPFC in goal-directed action control. In order to test the involvement of the vmPFC in goal-directed action control in the absence (versus presence) of cues, a first model crossed the trial type (cued for *valued* outcome, cued for *devalued* outcome, and *non-cued*) with the preferred response for each trial. Six separate regressors modelled valued (VALR) and devalued responses (DEVR) during the valued-cued (VAL), devalued-cued (DEV), and non-cued trials (NON). Nuisance regressors for the no-outcome condition and trials with missing responses were added separately. We hypothesized that the vmPFC tracks the outcome value of a response

in the context of non-cued trials, but not when this response is elicited by a Pavlovian cue (cued trials). Our interaction contrast focused therefore on brain activity related to preferring the valuable (versus devalued) response in the non-cued condition in comparison to preferring the valuable (versus devalued) response when it is driven by a compatible cue. The full contrast can be described as [NON-VALR minus NON-DEVR] minus [VAL-VALR minus DEV-DEVR].

We also tested whether vmPFC was generally more active during non-cued trials in comparison to cued trials (valued and devalued cues collapsed) regardless of the response preferred. To analyze this contrast we build a separate model that included regressors for each trial type that collapsed across valued and devalued responses. Nuisance regressors for the no-outcome condition and trials with missing responses were added separately.

Role of posterior putamen in outcome-specific transfer. In order to test whether posterior putamen is involved in outcome-specific PIT during the cued trials, we used the model that crossed trial type (valued, devalued and non-cued) with the preferred response, as specified above. In order to test the hypothesis that the posterior putamen is more active during responses compatible versus incompatible with the cue (as reported by Bray *et al.*, 2008), we computed the following contrast: [DEV-DEVR,VAL-VALR] minus [DEV-VALR,VAL-DEVR].

Functional connectivity between amygdala and posterior putamen during cued trials. In order to identify candidate neural structures that might show functional connectivity with posterior putamen, we first contrasted brain activity during cue presentation related to food outcomes versus no outcome, using the model that included each trial type and collapsed across valued and devalued responses, as specified above. This analysis revealed a region in the amygdala (see Results). Within this area we subsequently tested for differential functional connectivity with the posterior putamen (physiological variable) during compatible versus incompatible responses during cued trials (psychological variable) using a psychophysiological

interaction (PPI) model. The physiological regressor extracted time-course information based on a sphere (radius 8 mm) centered at the peak activation of posterior putamen (x = -30,y = -22, z = 4 mm; see Results).The convolved psychological regressor represented the contrast compatible trials minus incompatible trials, collapsed across the two food-related cues, i.e. [DEV-DEVR,VAL-VALR] minus [DEV-VALR,VAL-DEVR]. The PPI regressor was computed as the product of the demeaned physiological time course and the centered psychological regressor (O'Reilly *et al.*, 2012). **Note that the physiological regressor was not orthogonal to the psychological regressor because the regions used for the first was identified using the contrast that defined the latter. However, this is no reason for concern because we added the psychological regressor to the model, so the PPI regressor will detect functional connectivity effects over and above (orthogonal to) the psychological regressor (for a detailed explanation, see text and Figure 1 in O'Reilly *et al.*, 2012).** Following standard recommendations, a separate main effect regressor, i.e. [DEV-DEVR,VAL-VALR] plus [DEV-VALR,VAL-DEVR, was added in order to partition out shared variance. Nuisance regressors for the remaining trials were also modeled. Repeating the same approach, we also built a second PPI model that included the same physiological regressor but instead compared cued to non-cued trials (responses collapsed) as a psychological regressor.

DTI Preprocessing and Probabilistic Tracking

Standard FSL protocols for DTI preprocessing were followed including correction for susceptibility-induced distortions, brain extraction (manually checked and re-extracted if necessary), eddy correction, averaging of the two scans, and the fitting of diffusion tensors. Then diffusion parameters were sampled for each voxel using FSL bedpostX (Behrens *et al.*, 2007) which was followed by probabilistic tractography using FSL probtrackX (5000 samples;

curvature threshold, 0.2; no waypoint, exclusion, or termination masks; no advanced options) from within each participant's diffusion space. Following the approach described by Aarts and colleagues (Aarts *et al.*, 2012), we created seed-masks for the caudate and posterior putamen using automatic subcortical segmentation as implemented in FSL FIRST (Patenaude *et al.*, 2011). Individual masks were then transformed to standard space and for each individual the posterior putamen was delineated at $y < -1$ (Aarts *et al.*, 2012). Tracking was performed in diffusion space, after the seed masks were linearly transformed from standard space and visually inspected. Tractography results were then transformed back to standard space to produce a wholebrain image for each seed region, showing for each voxel the number of received samples. These individual 3D images were normalized for the size of the seed region and then merged into a single 4D file for statistical analyses.

VBM Preprocessing

FSL BET was applied to automate extraction of the brains from the T1 images, which were manually checked and re-extracted if not successful. FSL VBM tools (Smith *et al.*, 2004; Douaud *et al.*, 2007) with an optimized VBM protocol (Good *et al.*, 2001) were then used to create a study-specific gray matter template based on the individual T1 scans using non-linear registration. Following tissue-type segmentation, gray matter was registered to the standard MNI152 brain and then averaged across participants. Subsequently, individual participant gray matter images were then nonlinearly re-registered to the group template and smoothed using a Gaussian kernel of 4 mm. Finally, individual participants' 3D files were merged into a single 4D file for statistical analyses.

Specification of structural MRI analyses to test brain-structure hypotheses

To relate individual differences in behavior to structural differences in white matter tracts and gray matter integrity, we calculated a behavioral score of goal-directed behavior (mean number of valued responses minus mean number of devalued responses during the non-cued trials) and a behavioral score of outcome-specific transfer (mean number of compatible versus incompatible key presses during the valued and devalued cues). These two behavioral regressors were then demeaned and included in a model submitted to FSL randomise to assess significant positive voxel-wise correlations between the behavioral scores on the one hand and DTI and VBM data on the other hand. Because initial screening of these scores revealed that the index of goal-directed behavior was not normally distributed, this score was first transformed using log transformation (Shapiro-Wilk test of non-normality before transformation: $p < 0.001$, after transformation: $p = 0.463$).

Statistical Inference and Thresholding

For all functional and structural analyses, nonparametric voxelwise permutation-based statistical testing was performed using FSL randomise (5,000 permutations). In order to test our a priori hypotheses concerning the role of corticostriatal mechanisms, and to protect against false positives, analyses were constrained to small anatomically defined volumes of interest (these masks are depicted in blue in Figures 2-5). We used anatomical masks of the vmPFC (volume: 4593 voxels, 36,744 mm^3) that included medial orbitofrontal cortex and adjacent ventral medial cortex (combining rectus gyrus from the AAL atlas and frontal medial cortex from the FSL atlas, respectively) for the analyses concerning goal-directed action. We used a posterior-putamen mask (volume: 2120 voxels, 16,960 mm^3; putamen in FSL atlas delineated at $y < -1$), a premotor cortex mask (volume: 5970 voxels, 47,760 mm^3; juxtapositional lobule cortex in FSL atlas), and a bilateral amygdala mask (volume: 2967 voxels, 23,736 mm^3; amygdala in FSL atlas) for the

analyses concerning outcome-specific transfer. Only the analyses within these a-priori regions of interest are featured in the results. Given that our regions of interest contained relatively few voxels, for all analyses we used a significance criterion of $p < 0.01$ and a cluster extent threshold > 15 contiguous voxels (Cohen, Elger, & Weber, 2008), unless noted otherwise. In addition, DTI and VBM data were retained only for those voxels in which at least half of the participants had tracts to that voxel from the seed mask (using the same approach as de Wit *et al.*, 2012) and for those voxels that were part of the VBM template's gray matter mask, respectively. This further reduced the volume of interest and the associated chance to observe false positives. We present descriptive plots showing mean tractography and mean gray matter values of significant voxels correlated against the behavioral scores, using ranked scores that are robust against skewed distributions and outliers (Van den Brink *et al.*, 2014).

For reasons of completeness, we also report FSL's default (Smith & Nichols, 2009) threshold-free-cluster-enhanced and family-wise error corrected results confined to small volumes using a sphere of 8 mm centered at coordinates as reported in an earlier related study by Gläscher and colleagues (2009), see Results. For the interested reader, exploratory whole-brain analyses are presented in supplementary Table S1. These analyses use a threshold of $p < 0.001$ and a cluster threshold > 15 contiguous voxels. These whole-brain analyses should be considered preliminary and are not further discussed in this paper.

Results

Behavioral Results

A summary of the experimental design and behavioral results is presented in Figure 1.

Phase 1: Instrumental Training (R-O learning). All participants included in the behavioral analysis learned the correct R-O mapping. The average accuracy of R-O knowledge

assessed during the last block of query trials during this phase was 100%, for both the valued and the to-be devalued outcome.

Phase 2: Pavlovian Training (S-O learning). Participants learned the correct S-O mapping as the average accuracy of S-O knowledge assessed during the last block of query trials during this phase was 100% for the valued outcome and 97.7% (SD = 2.3 %) for the to-be devalued outcome. No main effect of satiation group nor interactions involving this factor were observed.

Phase 3: Satiation Manipulation. During TV watching, participants in the Smarties-satiation group ate on average 75g of chocolate Smarties (SD: 27g) and those in the popcorn-satiation group ate on average 43g of popcorn (SD: 13g). Figure 1B depicts the food desire ratings. As expected, repeated measures ANOVA on these ratings for the valued and devalued food before versus after the TV watching phase (T1 versus T2), revealed a significant interaction between Food value and Time, $F(1,20) = 66.5$, $MSE = 124.7$, $p < 0.001$. Follow-up t-tests showed that participants reported significantly less desire for the devalued food relative to the still-valuable food after satiation, $t(21) = 7.8$, $p < 0.001$, but not before, , $t(21) = 0.3$, $p = 0.769$. No main effect of satiation group nor further interactions involving this factor were observed. Additional repeated measures ANOVA on the hunger ratings before (T1, M = 46.0) and after satiation (T2, M = 32.0) revealed a reduction of hunger, $F(1,20) = 35.2$, $MSE = 61.3$, $p < 0.001$, and no effect of satiation group or interaction. Ratings of the TV show (M = 76.6) were not different for the two satiation groups ($F < 1$).

Phase 4: Non-cued and Cued Test Trials. The average number of presses to the four randomly-presented trial types in the test phase were submitted to a repeated-measures ANOVA with the factors response type (valued or devalued), trial type (non-cued, no-outcome, valued, or devalued) and satiation group (see Table 1 for the descriptive statistics). Analyses revealed a

main effect of response type, $F(1,20) = 5.2$, MSE = 22.3, $p = 0.034$, indicating an overall preference to respond more often with the key associated with the valued (unsatiated) outcome. There was also a main effect of trial type, $F(3,60) = 5.0$, MSE = 0.406, $p = 0.024$, and subsequent planned comparisons revealed overall lower response vigor (measured by the average number of key presses per trial) during the no-outcome cue versus the other three conditions (*p*s < 0.05). No main effect of satiation group, nor interactions involving this factor were observed. Most importantly, there was a significant interaction between response type and trial type, $F(3,60) = 25.7$, MSE = 11.4, $p < 0.001$. Subsequent ANOVAs were run to characterize responses specifically to the non-cued trials and the cued trials. All other factors remained the same.

Non-cued trials were analyzed to investigate goal-directed behavior (see Figure 1C, left panels). During non-cued trials, a main effect of response type was observed at statistical trend level, $F(1,20) = 3.3$, MSE = 11.9, $p = 0.084$, revealing a tendency to prefer the valued key (action selection based on value.). To further examine goal-directed action during non-cued trials, we assessed whether the difference score (number of valued responses minus number of devalued responses, ranked-transformed to correct for non-normality) during the non-cued trials was associated with an increased reduction of wanting of the devalued versus valued food (T2 wanting scores valued food minus T2 wanting scores devalued food). This was indeed the case. As is shown in Figure 1D (left scatterplot), participants who showed a stronger devaluation effects in terms of wanting also exhibited a reduced preference for the devalued response during the non-cued trials, $r(22) = 0.535$, $p = 0.010$.

Cued trials were analyzed to investigate outcome-specific (PIT) transfer (see Figure 1C, right panels). Consistent with earlier outcome-specific PIT findings, the ANOVA revealed an interaction between trial type (valued or devalued) and response, $F(1,20) = 38.2$, MSE = 22.7, $p < 0.001$, indicative of outcome-specific transfer. Subsequent t-tests, showed that there were more

compatible responses (i.e., responses associated with the outcome signaled by the cue) than incompatible responses (i.e., responses associated with outcomes other than that signaled by the cue) in response to both the valued cue, $t(21) = 6.9$, $p < 0.001$, and the devalued cue, $t(21) = 4.8$, $p < 0.001$. The analysis also revealed an interaction between trial type and satiation group, $F(1,20) = 6.6$, $MSE = 0.073$, $p = 0.018$. Subsequent analyses revealed that participants in the popcorn satiation group pushed generally more vigorously during the valued trials than the devalued trials , $F(1,10) = 15.5$, $MSE = 0.057$, $p = 0.003$, but this was not observed in the Smarties satiation group, $F(1,10) = 0.1$, $MSE = 0.090$, $p = 0.864$.

To investigate whether the degree of outcome-specific transfer was modulated by the value of the cue we calculated individual difference scores representing an increase in responding with the valued and devalued keys relative to performance in the non-cued trials (using the same approach as Watson et al., 2014). The ability of the cues to augment responding for the signaled outcome above the baseline response rate did not differ significantly between the valued and devalued cues, $t(21) = 1.5$, $p = 0.160$. In line with this insensitivity to value, the difference score (augmentation of valued minus devalued, ranked-transformed to correct for non-normality) was not correlated with the satiation effect on wanting (valued minus devalued food), $r(22) = -0.060$, $p = 0.790$ (Figure 1D, right scatterplot).

Summary of Main Behavioral Findings The behavioral patterns observed here (see Figure 1) replicated the results of the original paradigm developed by Watson and colleagues (Watson *et al.*, 2014). Following a successful instrumental and Pavlovian training phase, participants were satiated on one of the outcomes (popcorn or Smarties), which reduced their self-reported wanting for the sated outcome. In the subsequent test-phase (in the scanner), they were presented with cued and non-cued trials. During non-cued trials, participants tended to make more responses for the non-satiated (valued) outcome than responses for the satiated (devalued)

outcome. This effect correlated with the satiation-induced reduction of food wanting. In contrast, behavior during the cued trials was directed towards the outcome being signaled by the Pavlovian cue (indicating an outcome-specific transfer effect) and was not modulated by satiation.

Functional MRI Results

We analyzed BOLD data acquired during the test phase to investigate the neural computations that underlie the observed behavioral effects. We report separate analyses that focused on 1) the goal-directed responding in the non-cued versus cued trials, 2) the cue-driven responding during the cued (PIT) trials, and 3) functional connectivity during the cued trials.

Goal-directed Action Control in the Absence of Pavlovian Cues involves vmPFC. We first examined whether the preference for the valued response during the non-cued (versus cued) trials was associated with increased activity in the vmPFC. Specifically, we probed brain activity related to choosing the valuable (versus devalued) response in the non-cued condition, over and above brain activity related to choosing these valuable (versus devalued) responses when these are elicited by the cues. In other words, our interaction analysis probed for neural responses that track the action values in the absence of a cue while not being involved in tracking these action values in the presence of a cue (involving S→O→R associations). As shown in Figure 2, brain activation related to this action-value tracking was observed in the posterior vmPFC (x = 4,y = 28, z = -28 mm; p = 0.002; extent = 33 voxels). Activation in this region survived small volume correction (Family-wise error corrected $p<0.05$, using a sphere of 8mm centered at coordinates x=-6, y=24 z=-21 reported by Gläscher et al., 2009). An additional analysis constrained to the amygdala did not reveal clusters that met our significance criterion.

Brain activity was subsequently extracted from this region of the posterior vmPFC to plot and compare the four conditions that were involved in the contrast of interest (see Figure 2).

Planned comparisons revealed significantly increased activation when responding for the valued outcome in the non-cued condition relative to responding for the devalued outcome in both the non-cued ($p = 0.048$) and cued conditions ($p = 0.005$). The difference during responses directed towards valued and devalued outcomes in the cued condition was not significant ($p = 0.504$).

An additional analysis also probed for brain activity that was increased during all non-cued trials versus all valued and devalued cued trials. This analysis did not reveal clusters at our statistical threshold in the vmPFC.

Cue-driven Action Control (Outcome-specific PIT) during Cued Trials involves Posterior Putamen. In order to identify differential brain activity in posterior putamen related to outcome-specific transfer, we compared brain activity during trials in which participants performed the response compatible with the Pavlovian cue to trials in which participants performed the response incompatible with the Pavlovian cue, following the analysis reported by Bray and colleagues (2008). Consistent with the earlier observation by Bray and colleagues (2008), reduced brain activity to incompatible (versus compatible) responses, collapsed across the valued and devalued cues, was observed in the posterolateral putamen ($x = -30$, $y = -22$, $z = 4$ mm; $p < 0.001$; extent = 19 voxels) (see Figure 3A). The same analysis constrained to the amygdala did not reveal clusters that met our significance criterion.

The Role of the Amygdala in Cue-driven Outcome Representations. Given that cue-driven action control in our PIT paradigm was not sensitive to satiation, outcome-specific PIT is likely mediated mainly by the sensory (as opposed to hedonic) features of the outcome. In order to identify possible candidate neural structures that represent these sensory outcome features, we contrasted brain activity during cue presentation related to the food outcomes (collapsed across valued and devalued cues) versus no outcome. This analysis was focused on the vmPFC and amygdala. We found brain activity in a ventral region of the amygdala ($x = 34$, $y = 0$, $z = -28$

mm; p = 0.001; extent = 136 voxels, see Figure 3B, and x = -16, y = 2, z = -24 mm; p = 0.006; extent = 17 voxels), consistent with previous work that has implicated the ventral amygdala in specific PIT (Prevost *et al.*, 2012). A subsequent PPI analysis then confirmed that a similar region in ventral amygdala increased functional connectivity to the posterior putamen during compatible (versus incompatible) trials, albeit only at a lenient threshold of $p < 0.05$ (x = 12, y = -4, z = -22 mm; p = 0.008; extent = 71 voxels, see Figure 3C; overlap is displayed in Figure 3D). When we repeated this PPI analysis by comparing cued to non-cued trials, we found a similar cluster, again only when using a lenient statistical threshold of $p < 0.05$ (x = 22, y = -2, z = -26 mm; p = 0.008; extent = 86 voxels).

Structural MRI Results

vmPFC-striatal Connectivity Correlates with Individual Differences In Goal-directed Action Control. As illustrated in Figures 4A and 5A, and in line with earlier studies (Lehéricy *et al.*, 2004; Draganski *et al.*, 2008; de Wit *et al.*, 2012), white matter tracts from the caudate seed heavily projected to the vmPFC, whereas tracts from the posterior putamen seed innervated the premotor cortex. In order to test whether estimated tract strength in vmPFC voxels seeded from the caudate predicted goal-directed action, the behavioral score reflecting individual preference for valued responses over devalued responses during non-cued trials **(defined as the mean number of valued responses minus the mean number of devalued responses during the non-cued trials)** was correlated with the tractography results. This analysis revealed that the estimated strength of caudate-seeded white matter tracts to a vmPFC region (x = 4,y = 32, z = -18 mm; $p < 0.001$; extent = 32 voxels) (Figure 4B) that was significantly associated with increased goal-directed responding in the non-cued condition. The close proximity of the structural and functional data (compare Figure 2 and 4B) suggests that white matter tract innervations may

support the transmission of value information in the vmPFC to the caudate. To exclude the possibility that the area identified was also a predictor of cue-driven, habitual behavior, we ran a control analysis that investigated whether tract strength in this cluster was also related to the outcome-specific transfer score (defined as the mean number of compatible responses minus mean number of incompatible responses across the valued and devalued cues). The control analyses did not provide evidence for a significant association (ρs = 0.258 and 0.286, respectively), which suggests that the vmPFC cluster identified in the white-matter analysis is a unique predictor of goal-directed behavior specifically.

In order to test whether estimated tract strength in premotor cortex voxels seeded from the posterior putamen predicted PIT during the cued trials, we correlated tractography data with the score of outcome-specific transfer. This analysis revealed no clusters that met our significance criterion.

Gray Matter Density in Premotor Cortex Correlates with Individual Differences in Outcome-specific Pavlovian-Instrumental Transfer. To investigate whether differences in gray matter density in the vmPFC and the premotor cortex could predict goal-directed behavior and outcome-specific transfer, respectively, we ran a VBM analysis using the same two behavioral scores **(that is, the goal-directed behavior score and the** outcome-specific transfer score**)**. Although this analysis did not yield a positive correlation between gray matter density in the vmPFC and goal-directed behavior that met our significance criterion, we did observe a positive correlation between outcome-specific transfer and gray matter density in two clusters in the premotor cortex (x = -10,y = -6, z = 48 mm; $p < 0.001$; extent = 630 voxels and x = 0,y = 18, z = 68 mm; $p < 0.001$; extent = 141 voxels), as illustrated in Figure 5B. We also ran a control analysis that investigated whether local gray matter in the clusters identified by this analysis was also related to the goal-directed behavioral score. This was not the case ($\rho = 0.053$, $p = 0.829$),

which indicates that the gray matter observed in premotor cortex is a unique predictor of cued responding (outcome-specific PIT transfer) specifically.

Discussion

The present multimodal MRI study investigated corticostriatal activity and structure in relation to goal-directed versus cue-driven habitual food-seeking. To this end, we used a task in which instrumental responding to obtain popcorn or Smarties was assessed in the presence or absence of food-associated cues following satiation of one of these outcomes. This study is among the first to use satiation procedures to investigate the mechanisms of goal-directed and cue-driven food seeking in the human brain (Valentin *et al.*, 2007; Tricomi *et al.*, 2009; Tricomi & Lempert, 2015). Before turning to a discussion of the neural basis, we will first briefly summarize the main behavioral findings.

During non-cued trials, participants showed a tendency to preferentially respond for the non-satiated (valued) outcome, which was related to inter-individual variability in food desire/wanting ratings. This observation is consistent with earlier findings (Watson *et al.*, 2014) and with accounts of goal-directed behavior. In contrast, behavior during the cued trials was directed towards the outcome signaled by the Pavlovian cues independently of satiation, suggesting that it was controlled by the sensory – as opposed to the current hedonic features - of the outcome. These behavioral results replicated the findings observed in the original paradigm adopted by Watson and colleagues (Watson *et al.*, 2014). The fact that outcome-specific transfer was resistant to devaluation is in line with many other findings in both rodents (Colwill & Rescorla, 1990; Rescorla, 1994; Holland, 2004; Corbit *et al.*, 2007) and humans (Hogarth et al., 2012; Hogarth & Chase, 2011; but see Allman et al., 2010; Eder & Dignath, 2015). Our findings also resonate with dual-process models, which assume that behavior is controlled by goal-

directed and habitual mechanisms that operate in parallel (Dickinson *et al.*, 1995; de Wit & Dickinson, 2009; Balleine & O'Doherty, 2010; Hogarth & Chase, 2011; Huys *et al.*, 2011; Hogarth, 2012).

Neural mechanisms of goal-directed action

Our experimental design allowed us to identify a region in the vmPFC that was involved in goal-directed tracking specifically related to non-cued trials but not to cue-driven responding in the presence of a Pavlovian cue. In particular, we observed neural activity in a posterior part of the vmPFC that was increased when participants choose the valued response in the absence versus presence of an external cue. This observation makes an important contribution to earlier work that has implicated the vmPFC in representing the value of anticipated rewards, as observed in goal-directed behavior to obtain rewards (Arana *et al.*, 2003; O'Doherty *et al.*, 2003; Valentin *et al.*, 2007; de Wit *et al.*, 2009; Gläscher *et al.*, 2009) or when passively obtaining rewards during Pavlovian conditioning (O'Doherty *et al.*, 2002; Gottfried *et al.*, 2003). The observed increase in posterior vmPFC to responses associated with valued outcomes was specific for the non-cued trials and was absent in cued trials. Interestingly, this neural hotspot overlapped with a region of the vmPFC that Gläscher and colleagues (2009) have associated with tracking the expected outcome value of instrumental responses. Importantly, the value of the response during the cued trials was not tracked in this area (for related findings, see Balleine, Delgado, & Hikosaka, 2007; Gläscher et al., 2009; for caveats concerning the interpretation of null-findings, see O'Doherty, 2014).

Individual differences in the preference for responding on the key that predicted the valuable outcome were also related to structural integrity of the corticostriatal pathway that has been theorized to be involved in goal-directed action (Balleine & O'Doherty, 2010; de Wit *et al.*,

2012; Geurts *et al.*, 2013). To the best of our knowledge, we provide the first demonstration that behavior following satiation is related to individual variability in estimated white-matter tract strength between caudate and **a region of vmPFC that is in close proximity to the value-tracking brain region identified by the fMRI analysis.** Furthermore, the data presented here suggest that outcome-specific PIT is not related to this corticostriatal pathway, reinforcing the argument that goal-directed actions and cued responding are supported by distinct and dissociable networks.

Neural Mechanisms of Outcome-Specific Pavlovian-instrumental Transfer

During the outcome-specific PIT trials, neural activity in the posterior putamen was reduced when participants preferred responses that were incompatible with the action signaled by the cue. This observation is in line with the original finding reported by Bray and colleagues (2008) and has been interpreted to reflect the inhibition of O-R associations activated by the Pavlovian cue associated with reward.

The functional connectivity results provide new insights in how posterior putamen may receive input from neural structures that are involved in retrieving the sensory outcome associated with the cue. We observed increased functional coupling between the ventral amygdala and posterior putamen during outcome-compatible (versus incompatible) responses to the cue, an effect that is likely supported by well-documented anatomical amygdalostriatal connections between these areas (Zorrilla & Koob, 2013). Although this finding was only observed at a lenient statistical threshold, our findings are consistent with earlier work demonstrating that individuals with increased ventral amygdala activity show a stronger behavioral expression of outcome-specific transfer (Prevost *et al.*, 2012). These results are also consistent with lesion studies in animals that have implied the amygdalar basolateral complex in

the processing of the sensory features of an outcome (Corbit & Balleine, 2005; Balleine & Killcross, 2006; Talmi *et al.*, 2008).

We also investigated the possibility that individual differences in the anatomical tract connecting the posterior putamen and premotor cortex, thought to be involved in habitual behavior (Tricomi *et al.*, 2009; de Wit *et al.*, 2012; Liljeholm & O'Doherty, 2012), also predict outcome-specific PIT performance. However, although our fiber tracking results confirmed strong white-matter connectivity between posterior-putamen and premotor cortex (Lehéricy *et al.*, 2004; Draganski *et al.*, 2008; de Wit *et al.*, 2012), individual differences in this tract did not predict the strength of outcome-specific transfer. We did observe that gray matter integrity in the premotor cortex was a significant predictor of individual strength of outcome-specific transfer, suggesting that it plays a role in cue-elicited, outcome-insensitive behavior. In line with this finding, de Wit and colleagues (2012) have recently shown that gray matter in premotor cortex (next to posterior putamen) predicted habitual responding in an outcome-devaluation ('slips-of-action') task.

Societal/clinical relevance

Our findings provide further support that food-associated cues in the environment exert their influence on our behavior independently of satiation, by acting on the neural habit pathway. This line of research stresses the importance, therefore, of carefully regulating advertising aimed at selling unhealthy, high-calorie snacks – especially when aimed at children. In related research, we have demonstrated that these cueing effects are indeed stronger with high-calorie than with low-calorie snack cues in adolescents (Watson *et al.*, 2016). Combined with the demonstration that this associative (PIT) mechanism is not flexibly modulated by changes in motivation (e.g.,

through satiation), these studies suggest that food-associated cues in our obesogenic environment may play a central role in overeating and in the increased prevalence of overweight.

Limitations

We mention a few limitations of the present study. First, the majority of participants in our study were female and we did not control for their menstrual cycle phase. Given that menstrual cycle affects reward processing (Dreher *et al.*, 2007) it could have increased variance in our estimates of goal-directed and habitual behavior. Thus, it is possible that we have actually underestimated the strengths of the relationship between individual differences in behavior and brain structure. Further, we could not determine the role of gender differences in the present study due to the small number of males (N=4) in our analyses. Second, most of the neuroimaging results reported were significant at a lenient statistical threshold only, although we aimed to protect against false positives by using small a-priori defined volumes of interest. Finally, some of the analyses could include no more than 11 participants, thus reducing the power to detect possible effects. However, it is important to emphasize that our main results, even for the analysis using a small sample size, confirmed observations from earlier studies and that our results convergence considerably across the three different modalities (fMRI, DTI and gray matter) analyzed in the present study.

Conclusions

Using a satiation procedure in combination with a PIT task, this multimodal MRI study showed for the first time that a region in the posterior vmPFC uniquely tracks the value of goal-directed actions (in the absence of external cues) while not tracking this value when the same action is elicited by a Pavlovian cue. Additional functional and structural analyses provided

converging evidence for earlier findings (Valentin *et al.*, 2007; Talmi *et al.*, 2008; de Wit *et al.*, 2009, 2012; Prevost *et al.*, 2012) and theories suggesting that goal-directed action and outcome-specific PIT tap into dissociable mechanisms involving the vmPFC-caudate and putamen-premotor cortex network, respectively (Balleine & O'Doherty, 2010). More generally, our results add to existing evidence that reward-associated cues can direct behavior, even when the outcome is not currently desired. Such habit-like responding may play an important role in the development of addiction to food, but also drugs (Ludwig *et al.*, 1974; Everitt & Robbins, 2005). The current work contributes to a fundamental understanding of the brain circuits involved in goal-directed and cue-driven food seeking which might, ultimately, also help to improve existing treatments to change maladaptive cue-driven behavior.

Abbreviations

diffusion tensor imaging (DTI)

functional magnetic resonance imaging (fMRI)

Inter-trial interval (ITI)

Pavlovian-instrumental transfer (PIT)

psychophysiological interaction (PPI)

ventromedial prefrontal cortex (vmPFC)

voxel-based morphometry (VBM)

References

Aarts, E., Helmich, R.C., Janssen, M.J.R., Oyen, W.J.G., Bloem, B.R., & Cools, R. (2012) Aberrant reward processing in Parkinson's disease is associated with dopamine cell loss. *Neuroimage*, **59**, 3339–3346.

Adams, C.D. (1982) Variations in the sensitivity of instrumental responding to reinforcer devaluation. *Q. J. Exp. Psychol.*, **34**, 77–98.

Allman, M.J., Deleon, I.G., Cataldo, M.F., Holland, P.C., & Johnson, A.W. (2010) Learning processes affecting human decision making: An assessment of reinforcer-selective pavlovian-to-instrumental transfer following reinforcer devaluation. *J. Exp. Psychol. Behav. Process.*, **36**, 402–408.

Arana, F.S., Parkinson, J.A., Hinton, E., Holland, A.J., Owen, A.M., & Roberts, A.C. (2003) Dissociable contributions of the human amygdala and orbitofrontal cortex to incentive motivation and goal selection. *J. Neurosci.*, **23**, 9632–9638.

Balleine, B.W. & Killcross, S. (2006) Parallel incentive processing: an integrated view of amygdala function. *Trends Neurosci.*, **29**, 272–279.

Balleine, B.W. & O'Doherty, J.P. (2010) Human and rodent homologies in action control: corticostriatal determinants of goal-directed and habitual action. *Neuropsychopharmacology*, **35**, 48–69.

Behrens, T.E.J., Berg, H.J., Jbabdi, S., Rushworth, M.F.S., & Woolrich, M.W. (2007) Probabilistic diffusion tractography with multiple fibre orientations: What can we gain? *Neuroimage*, **34**, 144–155.

Bray, S., Rangel, A., Shimojo, S., Balleine, B., & O'Doherty, J.P. (2008) The neural mechanisms underlying the influence of pavlovian cues on human decision making. *J. Neurosci.*, **28**, 5861–5866.

Colwill, R.M. & Rescorla, R.A. (1985) Instrumental responding remains sensitive to reinforcer devaluation after extensive training. *J. Exp. Psychol. Anim. Behav. Process.*, **11**, 520.

Colwill, R.M. & Rescorla, R.A. (1988) The role of response-reinforcer associations increases throughout extended instrumental training. *Anim. Learn. Behav.*, **16**, 105–111.

Colwill, R.M. & Rescorla, R.A. (1990) Effect of reinforcer devaluation on discriminative control of instrumental behavior. *J. Exp. Psychol. Anim. Behav. Process.*, **16**, 40.

Corbit, L.H. & Balleine, B.W. (2005) Double dissociation of basolateral and central amygdala lesions on the general and outcome-specific forms of pavlovian-instrumental transfer. *J. Neurosci.*, **25**, 962–970.

Corbit, L.H., Janak, P.H., & Balleine, B.W. (2007) General and outcome-specific forms of Pavlovian-instrumental transfer: the effect of shifts in motivational state and inactivation of the ventral tegmental area. *Eur. J. Neurosci.*, **26**, 3141–3149.

de Wit, S., Corlett, P.R., Aitken, M.R.F., Dickinson, A., & Fletcher, P.C. (2009) Differential engagement of the ventromedial prefrontal cortex by goal-directed and habitual behavior toward food pictures in humans. *J. Neurosci.*, **29**, 11330–11338.

de Wit, S. & Dickinson, A. (2009) Associative theories of goal-directed behaviour: a case for

animal-human translational models. *Psychol. Res.*, **73**, 463–476.

de Wit, S., Watson, P., Harsay, H.A., Cohen, M.X., van de Vijver, I., & Ridderinkhof, K.R. (2012) Corticostriatal connectivity underlies individual differences in the balance between habitual and goal-directed action control. *J. Neurosci.*, **32**, 12066.

Delamater, A.R. & Oakeshott, S. (2007) Learning about multiple attributes of reward in Pavlovian conditioning. *Ann. N. Y. Acad. Sci.*, **1104**, 1–20.

Delorme, C., Salvador, A., Valabrègue, R., Roze, E., Palminteri, S., Vidailhet, M., de Wit, S., Robbins, T., Hartmann, A., & Worbe, Y. (2016) Enhanced habit formation in Gilles de la Tourette syndrome. *Brain*, **139**, 605–615.

Dickinson, A., Balleine, B., Watt, A., Gonzalez, F., & Boakes, R.A. (1995) Motivational control after extended instrumental training. *Anim. Learn. Behav.*, **23**, 197–206.

Douaud, G., Smith, S.M., Jenkinson, M., Behrens, T., Johansen-Berg, H., Vickers, J., James, S., Voets, N., Watkins, K., & Matthews, P.M. (2007) Anatomically related grey and white matter abnormalities in adolescent-onset schizophrenia. *Brain*, **130**, 2375–2386.

Draganski, B., Kherif, F., Klöppel, S., Cook, P. a, Alexander, D.C., Parker, G.J.M., Deichmann, R., Ashburner, J., & Frackowiak, R.S.J. (2008) Evidence for segregated and integrative connectivity patterns in the human Basal Ganglia. *J. Neurosci.*, **28**, 7143–7152.

Dreher, J.-C., Schmidt, P.J., Kohn, P., Furman, D., Rubinow, D., & Berman, K.F. (2007) Menstrual cycle phase modulates reward-related neural function in women. *Proc. Natl. Acad. Sci.*, **104**, 2465–2470.

Eder, A.B. & Dignath, D. (2015) Cue-elicited food seeking is eliminated with aversive outcomes following outcome devaluation. *Q. J. Exp. Psychol.*, 1–15.

Everitt, B.J. & Robbins, T.W. (2005) Neural systems of reinforcement for drug addiction: from actions to habits to compulsion. *Nat. Neurosci.*, **8**, 1481–1489.

Geurts, D.E.M., Huys, Q.J.M., den Ouden, H.E.M., & Cools, R. (2013) Aversive pavlovian control of instrumental behavior in humans. *J. Cogn. Neurosci.*, **25**, 1428–1441.

Gläscher, J., Hampton, A.N., & O'Doherty, J.P. (2009) Determining a role for ventromedial prefrontal cortex in encoding action-based value signals during reward-related decision making. *Cereb. Cortex*, **19**, 483–495.

Good, C.D., Johnsrude, I.S., Ashburner, J., Henson, R.N.A., Fristen, K.J., & Frackowiak, R.S.J. (2001) A voxel-based morphometric study of ageing in 465 normal adult human brains. *Neuroimage*, **14**, 21–36.

Gottfried, J.A., O'Doherty, J.P., & Dolan, R.J. (2003) Encoding predictive reward value in human amygdala and orbitofrontal cortex. *Science (80-.).*, **301**, 1104–1107.

Heyes, C. & Dickinson, A. (1990) The intentionality of animal action. *Mind Lang.*, **5**, 87–103.

Hogarth, L. (2012) Goal-directed and transfer-cue-elicited drug-seeking are dissociated by pharmacotherapy: Evidence for independent additive controllers. *J. Exp. Psychol. Anim. Behav. Process.*, **38**, 266–278.

Hogarth, L. & Chase, H.W. (2011) Parallel goal-directed and habitual control of human drug-seeking: implications for dependence vulnerability. *J. Exp. Psychol. Anim. Behav. Process.*, **37**, 261–276.

Hogarth, L., Chase, H.W., & Baess, K. (2012) Impaired goal-directed behavioural control in human impulsivity. *Q. J. Exp. Psychol. (Hove).*, **65**, 305–316.

Holland, P.C. (2004) Relations between Pavlovian-instrumental transfer and reinforcer devaluation. *J. Exp. Psychol. Anim. Behav. Process.*, **30**, 104.

Hommel, B. (2015) Goal-directed actions. In Waldmann, M. (ed), *Handbook of Causal Reasoning*. Oxford University Press, Oxford, England, pp. 1–34.

Huys, Q.J.M., Cools, R., Gölzer, M., Friedel, E., Heinz, A., Dolan, R.J., Dayan, P., Golzer, M., Friedel, E., Heinz, A., Dolan, R.J., & Dayan, P. (2011) Disentangling the roles of approach, activation and valence in instrumental and pavlovian responding. *Plos Comput. Biol.*, **7**, e1002028.

Lehéricy, S., Ducros, M., Van De Moortele, P.F., Francois, C., Thivard, L., Poupon, C., Swindale, N., Ugurbil, K., & Kim, D.S. (2004) Diffusion tensor fiber tracking shows distinct corticostriatal circuits in humans. *Ann. Neurol.*, **55**, 522–529.

Liljeholm, M. & O'Doherty, J.P. (2012) Contributions of the striatum to learning, motivation, and performance: an associative account. *Trends Cogn. Sci.*, **16**, 467–475.

Ludwig, A.M., Wikler, A., & Stark, L.H. (1974) The first drink: Psychobiological aspects of craving. *Arch. Gen. Psychiatry*, **30**, 539–547.

O'Doherty, J.P. (2014) The problem with value. *Neurosci. Biobehav. Rev.*, **43**, 259–268.

O'Doherty, J.P., Critchley, H., Deichmann, R., & Dolan, R.J. (2003) Dissociating valence of outcome from behavioral control in human orbital and ventral prefrontal cortices. *J. Neurosci.*, **23**, 7931–7939.

O'Doherty, J.P., Deichmann, R., Critchley, H.D., & Dolan, R.J. (2002) Neural responses during anticipation of a primary taste reward. *Neuron*, **33**, 815–826.

O'Reilly, J.X., Woolrich, M.W., Behrens, T.E.J., Smith, S.M., & Johansen-Berg, H. (2012) Tools of the trade: Psychophysiological interactions and functional connectivity. *Soc. Cogn. Affect. Neurosci.*, **7**, 604–609.

Patenaude, B., Smith, S.M., Kennedy, D.N., & Jenkinson, M. (2011) A Bayesian model of shape and appearance for subcortical brain segmentation. *Neuroimage*, **56**, 907–922.

Prevost, C., Liljeholm, M., Tyszka, J.M., O'Doherty, J.P., Prévost, C., Liljeholm, M., Tyszka, J.M., O'Doherty, J.P., Prevost, C., Liljeholm, M., Tyszka, J.M., & O'Doherty, J.P. (2012) Neural Correlates of Specific and General Pavlovian-to-Instrumental Transfer within Human Amygdalar Subregions: A High-Resolution fMRI Study. *J. Neurosci.*, **32**, 8383–8390.

Rescorla, R.A. (1994) Transfer of instrumental control mediated by a devalued outcome. *Anim. Learn. Behav.*, **22**, 27–33.

Smith, S.M., Jenkinson, M., Woolrich, M.W., Beckmann, C.F., Behrens, T.E.J., Johansen-Berg, H., Bannister, P.R., De Luca, M., Drobnjak, I., Flitney, D.E., Niazy, R.K., Saunders, J., Vickers, J., Zhang, Y.Y., De Stefano, N., Brady, J.M., & Matthews, P.M. (2004) Advances in functional and structural MR image analysis and implementation as FSL. *Neuroimage*, **23**, S208–S219.

Smith, S.M. & Nichols, T.E. (2009) Threshold-free cluster enhancement: addressing problems of smoothing, threshold dependence and localisation in cluster inference. *Neuroimage*, **44**, 83–

98.

Talmi, D., Seymour, B., Dayan, P., & Dolan, R.J. (2008) Human pavlovian-instrumental transfer. *J. Neurosci.*, **28**, 360–368.

Tricomi, E., Balleine, B.W., & O'Doherty, J.P. (2009) A specific role for posterior dorsolateral striatum in human habit learning. *Eur. J. Neurosci.*, **29**, 2225–2232.

Tricomi, E. & Lempert, K.M. (2015) Value and probability coding in a feedback-based learning task utilizing food rewards. *J. Neurophysiol.*, **113**, 4–13.

Valentin, V. V, Dickinson, A., & O'Doherty, J.P. (2007) Determining the neural substrates of goal-directed learning in the human brain. *J. Neurosci.*, **27**, 4019–4026.

Van den Brink, R.L., Cohen, M.X., van der Burg, E., Talsma, D., Vissers, M.E., & Slagter, H. a. (2014) Subcortical, modality-specific pathways contribute to multisensory processing in humans. *Cereb. Cortex*, **24**, 2169–2177.

Watson, P., Wiers, R.W., Hommel, B., & de Wit, S. (2014) Working for food you don't desire – cues interfere with goal-directed food-seeking. *Appetite*, **79**, 139–148.

Watson, P., Wiers, R.W., Hommel, B., Ridderinkhof, K.R., & de Wit, S. (2016) An associative account of how the obesogenic environment biases adolescents' food choices. *Appetite*, **96**, 560–571.

Zorrilla, E.P. & Koob, G.F. (2013) Amygdalostriatal projections in the neurocircuitry for motivation: a neuroanatomical thread through the career of Ann Kelley. *Neurosci. Biobehav. Rev.*, **37**, 1932–1945.

Table 1. Behavioral Data Test Phase

Satiation group	Trial type	Average number of key presses			
		Valued key		Devalued key	
		Mean	SD	Mean	SD
Participants satiated on popcorn (N=11)	non-cued	6.36	4.66	3.41	2.53
	cued no-outcome	6.06	3.61	3.04	2.05
	cued devalued outcome	2.41	3.10	7.08	4.08
	cued valued outcome	8.51	4.55	1.55	1.59
Participants satiated on Smarties (N=11)	non-cued	6.00	2.00	5.16	1.83
	cued no-outcome	5.73	3.20	4.75	1.97
	cued devalued outcome	2.60	2.44	8.95	2.99
	cued valued outcome	9.32	3.10	2.20	1.95

Figures

FIGURE 1

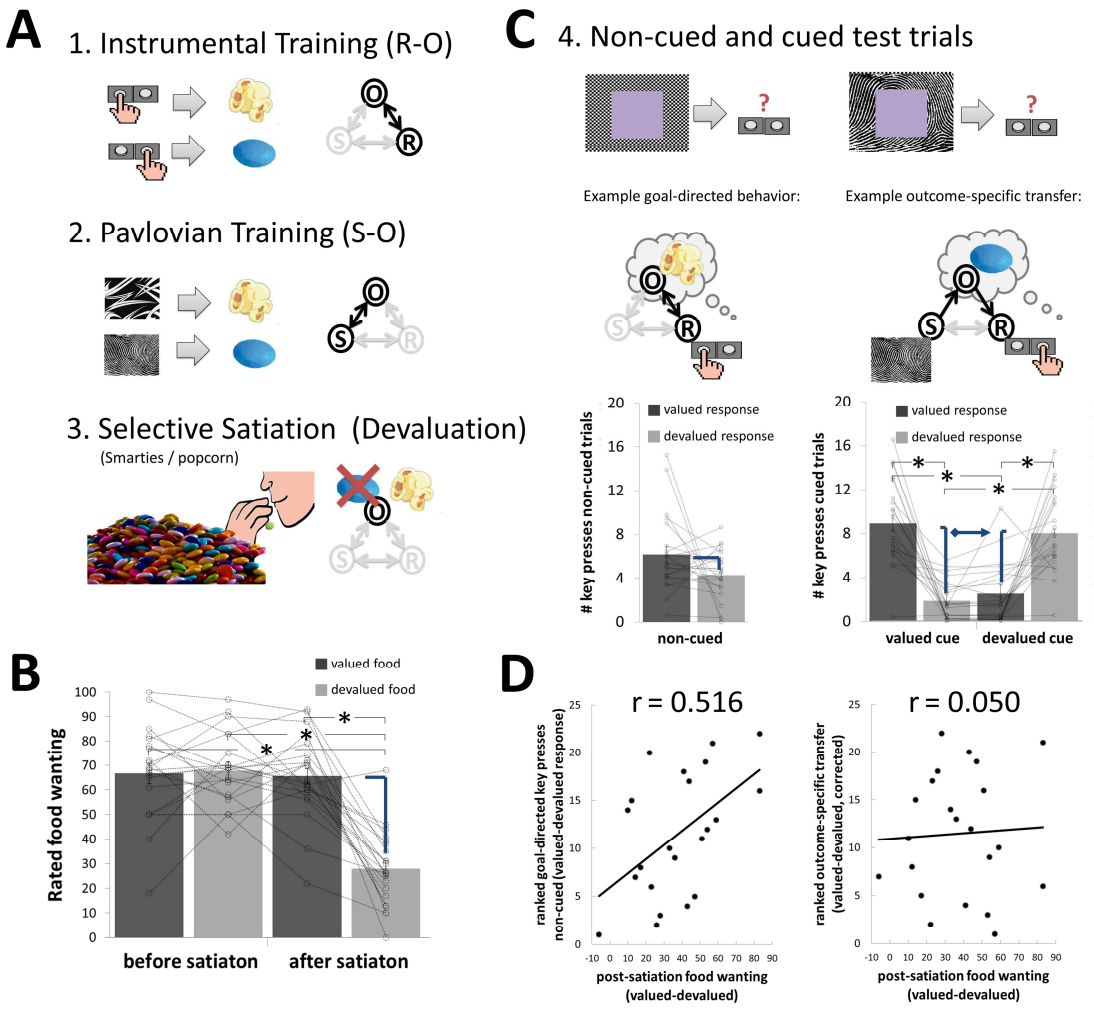

Figure 1. Overview of the experimental design and behavioral results. **A.** Outside the scanner, participants first learned the association between two responses and two food-outcomes (Smarties or popcorn), followed by a Pavlovian phase in which two stimuli were associated with the outcomes. Another stimulus was associated with no outcome (not shown in the figure). Participants were then satiated on either Smarties or popcorn. **B.** Food desire was reduced following satiation (devaluation) of the specific outcome. **C.** During the test phase in the scanner, participants were presented with intermixed non-cued and cued test trials. In the absence of a cue (non-cued trials), participants made more key presses for the valued response. In the presence of a cue participants preferred responses that were compatible with the outcome predicted by the cue, irrespective of whether the outcome was valued or devalued. **D.** Post-satiation food desire (indicated in blue in B) was correlated with the behavioral preference score for the valued response during the non-cued trials (indicating goal-directed behavior) and was not correlated with the outcome-specific transfer score (indicated in blue in C and baseline corrected, see Results). Note: Bar graphs in B and C show means and standard errors and lines show data from individual participants. Significant differences ($p < .05$) between cell means are indicated by asterisks.

FIGURE 2

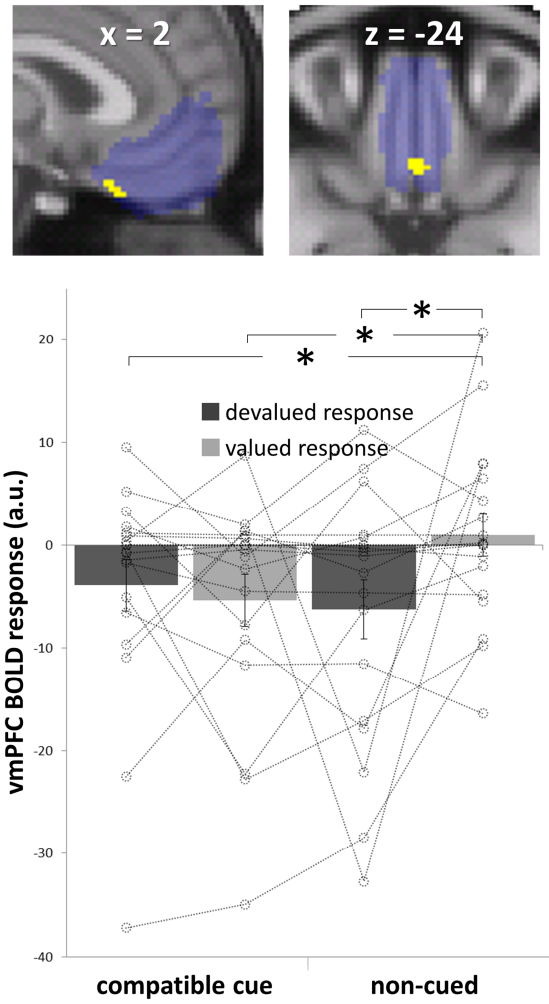

Figure 2. Activation in the posterior vmPFC related to goal-directed behavior - choosing the valuable (versus devalued) response in the non-cued condition in comparison to the same choice in the context of a compatible cue: [NON-VALR minus NON-DEVR] minus [VAL-VALR minus DEV-DEVR]. Analyses restricted to the a-prior region of interest (depicted in blue). Thresholded at $p < 0.01$, > 15 contiguous voxels. Left side of the axial image corresponds to the right side of the brain.The bar graph shows means and standard errors and lines show data from individual participants.

FIGURE 3

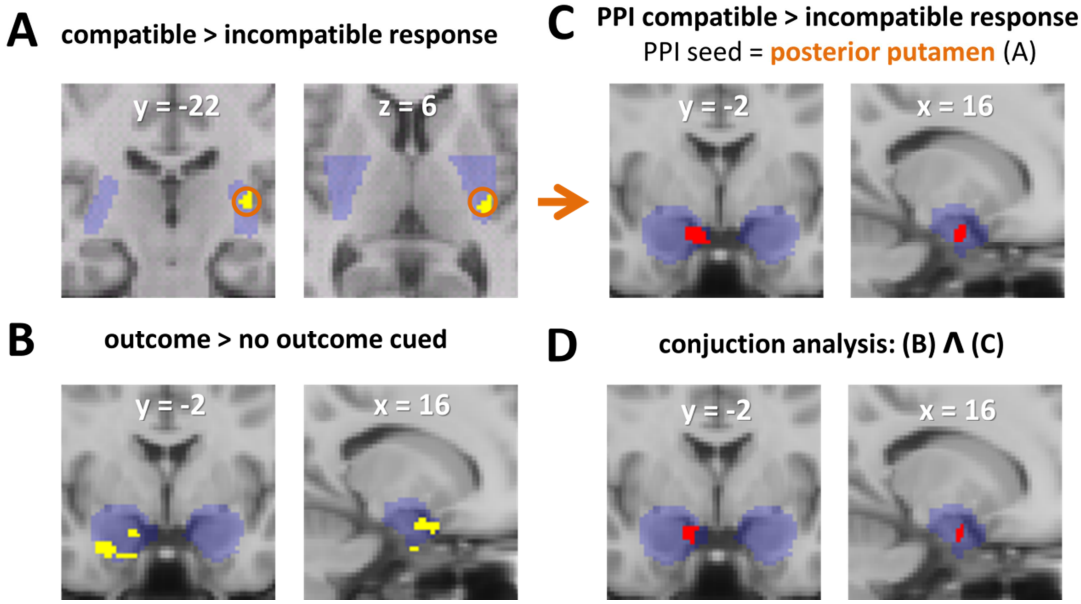

Figure 3. Functional MRI analyses of outcome-specific transfer. All analyses restricted to the a-prior region of interest (depicted in blue). Left side of the coronal and axial images corresponds to the right side of the brain. **A.** Brain activity in the posterior putamen during outcome-specific transfer - compatible minus incompatible responses collapsed across valued and devalued cues. Thresholded at $p < 0.01$, > 15 contiguous voxels. **B.** Ventral amygdala as candidate brain region for cue-driven outcome processing – food-outcome cues minus no-outcome cue. Thresholded at $p < 0.01$, > 15 contiguous voxels. **C. PPI analysis.** Increased functional connectivity between posterior putamen seed (depicted in A) and amygdala during compatible versus incompatible responses. Thresholded at $p < 0.05$. **D.** Conjunction analysis of the contrasts in (B) and (C) showing partial overlap. Thresholded at $p < 0.05$.

FIGURE 4

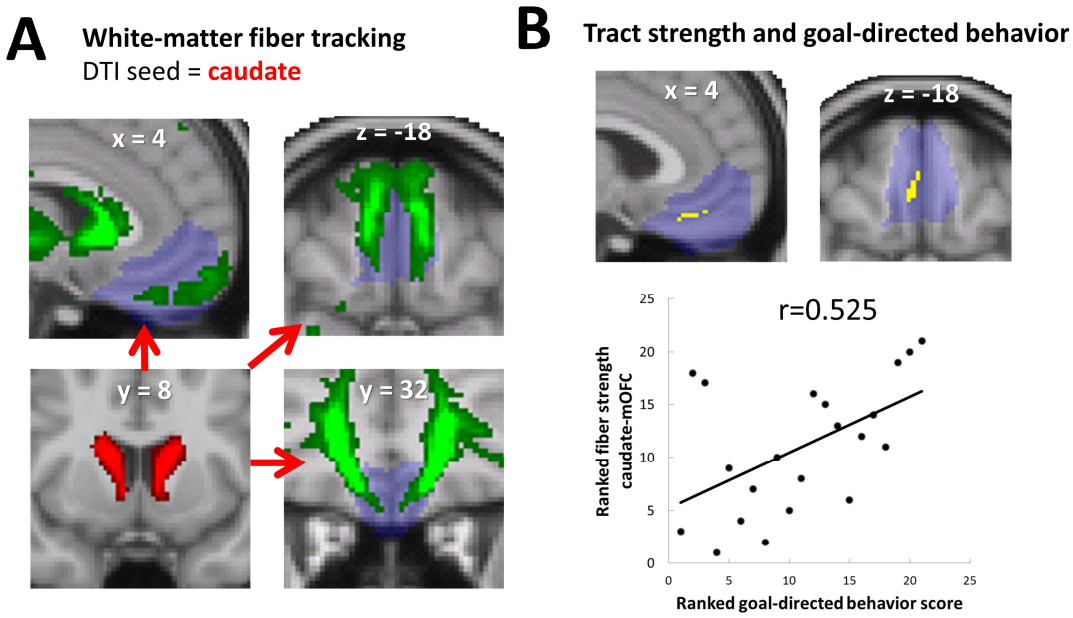

Figure 4. DTI and goal-directed behavior during the non-cued trials. **A.** Raw tractography results depicted in green: Caudate seed (depicted in red) projections to vmPFC (thresholded at 0.05% of average total samples sent). **B.** Estimated white matter tract strength between caudate seed and vmPFC significantly predicted goal-directed behavior during the non-cued test trials. Analyses restricted to a-priori region of interest (depicted in blue). Thresholded at $p < 0.01$, > 15 contiguous voxels. Left side of the coronal and axial images corresponds to the right side of the brain.

.

FIGURE 5

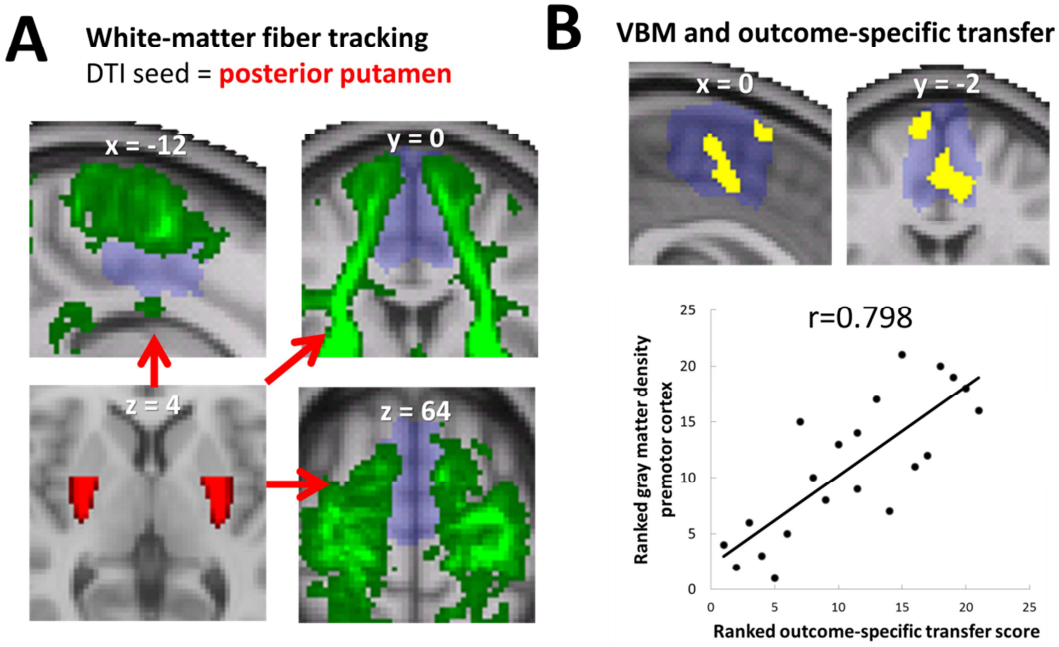

Figure 5. DTI and outcome-specific transfer (cued test trials). **A.** Raw tractography results depicted in green: Posterior putamen seed depicted in red) projections to premotor cortex (thresholded at 0.05% of average total samples sent). Tract strength did not correlate with behavior (see text) **B.** VBM and outcome-specific Pavlovian-instrumental transfer. Gray matter integrity of the premotor cortex predicted individual outcome-specific transfer scores. Analyses restricted to the a-priori region of interest (depicted in blue). Thresholded at $p < 0.01$, > 15 contiguous voxels. Left side of the coronal and axial images corresponds to the right side of the brain.

SUPPLEMENTARY MATERIAL

Table S1. Explorative whole-brain analyses

Analysis	Area	Cluster size (voxels)	Peak MNI coordinates (X Y Z)		
BOLD goal-directed action control	Temporal Occipital Fusiform Cortex	67	-36	-52	-4
	Hippocampus	47	-20	-44	6
		35	36	-22	-16
BOLD cue-driven action control	Lateral occipital cortex,Precuneous Cortex	241	-38	-52	6
		153	10	-64	54
		131	-12	-68	52
	Heschl's Gyrus, Opercular Cortex	111	-38	-28	8
	Superior Frontal Gyrus	50	24	-8	66
BOLD valued/devalued > non-cued	Lateral Occipital Cortex, Occipital Pole, Occipital Fusiform Gyrus, Lingual Gyrus, Cuneal Cortex, Temporal Occipital Fusiform Cortex	8784	38	-48	-22
	Caudate	74	26	-16	18
	Caudate	37	-2	18	4
	Frontal Polar Cortex	33	-16	52	20
BOLD outcome > no outcome cued	Frontal Polar Cortex	83	-14	66	-6
VBM positive correlation with cue-driven action-control	Middle Temporal Gyrus, Lateral Occipital Cortex	142	-64	-56	2
	Occipital Pole	140	32	-92	2
	Precuneous Cortex, Postcentral Gyrus	61	-2	-52	60
	Premotor Cortex	26	14	-12	66
	Postcentral Gyrus, Supramarginal Gyrus	18	-58	-26	48
	Superior Frontal Gyrus	16	0	18	68

Note: reported clusters are thresholded at $p < 0.001$ and a cluster extend > 15 contiguous voxels